Comparative study of model potentials for the calculation of dielectric properties of small metal particles

W. Ekardt

Solid State Division, Oak Ridge National Laboratory, Oak Ridge, Tennessee 37831
and Fritz-Haber-Institut der Max-Planck-Gesellschaft, Faradayweg 4-6, D-1000 Berlin 33, Federal Republic of Germany

Z. Penzar

Fritz-Haber-Institut der Max-Planck-Gesellschaft, Faradayweg 4-6, D-1000 Berlin 33, Federal Republic of Germany
and Institute of Physics of the University, P.O. Box 304, YU-41001 Zagreb, Croatia, Yugoslavia

M. Šunjić

Department of Physics, Faculty of Science, P.O. Box 162, YU-41001 Zagreb, Croatia, Yugoslavia

Quite recently the dielectric electronic-response properties of small metal particles were investigated within a strictly self-consistent spherical jellium model. The bottleneck of this kind of calculation for a larger cluster is the self-consistent solution of the single-electron Kohn-Sham equations. Therefore, in this work simple model potentials are investigated and compared with the Kohn-Sham barrier. The result of this comparison is that the widely used model potentials such as finite- or infinite-step potentials are not able to mimic the complex dynamical behavior of a fully self-consistently responding surface.

I. INTRODUCTION

Quite recently a number of authors started investigating the dielectric properties of small metal particles at a strictly microscopic level.[1-8] The model used in all of these investigations was the self consistent spherical jellium model, and the concept used to describe the response properties was the time-dependent local-density approximation (TDLDA) due to Zangwill and Soven[9] and Stott and Zaremba.[10]

A major problem to apply this method consists in the self-consistent solution of the Kohn-Sham equations[6,11-13] for a larger number of electrons (say, beyond 500 valence electrons of sodium) describing the ground state of the system. Therefore, one very often tries to avoid this time-consuming computational work either by the application of quasiclassical concepts such as the semiclassical infinite-barrier model (SCIB),[14,15] or by applying the quantum-infinite-barrier (QIB) model,[16,17] or even other models such as the hydrodynamical model,[18] the sum rule technique,[19] and the statistical method.[20]

In this paper we adopt a different approach. Because of our knowledge of the exact results (within a spherical jellium model) both concerning the *dipolar* response[1-7] and concerning the response properties of the *higher multipoles*,[8] we are now in a better position. Using the exact results as a bench mark, we simply study a number of popular model potentials confining the electronic motion within a spherical particle and look at the results. In *this* paper we investigate three different *step* potentials as the simplest way to describe electronic localization within a sphere. The motivation for doing so is as follows. We know from the current literature that both for planar jelli-

um surfaces[21] and for spherical ones[22] a steplike single-particle potential gives rather accurate ground-state properties provided that step height and edge position (with respect to the jellium background) are determined by minimizing the ground-state energy functional. Hence, it is tempting to use the single-particle potential obtained in this way for the calculation of the various ingredients needed for the application of the TDLDA. As we shall see below, this procedure yields reasonable results as far as the *static* polarizability is concerned (this outcome is, of course, *not* surprising; nevertheless, it is a new result), whereas the dynamical response, of course, deviates considerably from the corresponding Kohn-Sham behavior.

Therefore, we investigated in a second step another step potential which was especially designed to reproduce the *dynamical* behavior. This potential is *not* sanctioned by any minimization principle. Its parameters are simply determined to give a best fit to the occupied part of the (known) Kohn-Sham single-particle level scheme. As expected, the dynamical polarizabilities compare now better with the corresponding Kohn-Sham results, but not as well as one might think.

Finally, we present the various dynamical multipole properties of the quantum-infinite-barrier model. The result here is similar to what is known for the planar jellium surface. The QIB possesses so many intrinsic flaws that it should no longer be used, at least insofar as one believes in the relevance of the Kohn-Sham barrier.

The rest of the paper is organized as follows: In Sec. II we present the ground-state potentials and charge densities and compare them with the corresponding Kohn-Sham properties. Section III gives a short summary of the TDLDA formalism as used in this paper. Section IV contains the static response properties, whereas Sec. V

gives a detailed account of the dynamical properties. Section VI is the conclusion.

II. MODEL POTENTIALS

The most straightforward reasonable step potential which can be used in any type of response calculation would be that potential minimizing the total energy of the system. This would mean that we are constructing a model which is completely analogous to the original TDLDA except for the missing self-consistency. Such a potential is sanctioned by the minimization principle and, therefore, its parameters are in no way arbitrarily fixed. For that reason we studied this potential first. The starting point to obtain this potential is completely the same as in the exact Kohn-Sham theory. The variation of the total energy functional $E[\rho]$,

$$E[\rho]=E_{\text{kin}}[\rho]+E_{\text{xc}}[\rho]+E_{\text{es}}[\rho] , \tag{1}$$

with respect to the electronic density $\rho(r)$, leads directly to the Kohn-Sham equations,

$$[-\Delta+V(r;\rho(r))]\Psi_i(r)=\epsilon_i\Psi_i(r) , \tag{2}$$

which, however, are not solved self-consistently. On the contrary, the potential $V(r;\rho(r))$ is replaced by a finite-step potential

$$V(r;\rho(r))\Longrightarrow -V_0\Theta(R_0-r) , \tag{3}$$

which makes Eq. (2) analytically tractable. The wave functions $\Psi_i(r)$ depend parametrically on V_0 and R_0, and so does the density $\rho(r)$ and the total energy $E[\rho]$. Hence the best potential within the family of trial potentials, Eq. (3), is easily found by searching for E_{min}. The input data needed for this model are the same as for the corresponding Kohn-Sham problem, namely the jellium density r_s and the number of valence electrons N to be considered. This gives, via $R_J=N^{1/3}r_s$, the jellium background radius R_J. We performed these calculations for a variety of particle numbers in the case of $r_s=4$ and reproduced (with slight modifications) the results concerning the ionization potential already published in the literature.[22] At the same time we looked at the convergency of V_0 and R_0 toward their known semi-infinite half-space values.[21] The convergence is slow but takes place.

We show in Fig. 1 a plot of the charge density and the single particle levels in the case of $r_s=4$ and $N=92$. The value of V_0 in that case is $V_0=0.2889$ Ry and the radius of the potential R_0, is given by $R_0=18.365$ a.u. (compared to $R_J=18.057$ a.u.). The charge density looks indeed very similar to the corresponding Kohn-Sham charge density, shown in Fig. 2, whereas the potential looks rather different. It is considerably shallower than the Kohn-Sham potential Fig. 2. This result qualitatively agrees with what has been found by Rose and Shore[21] for the semi-infinite half-space. As we shall see later, it is mainly this shallowness which makes the dynamical response so different from the Kohn-Sham response.

Another potential whose response properties we investigated is the one with depth and width simply used as fitting parameters to reproduce the occupied part of the Kohn-Sham single-particle level scheme. For $V_0=0.4413$
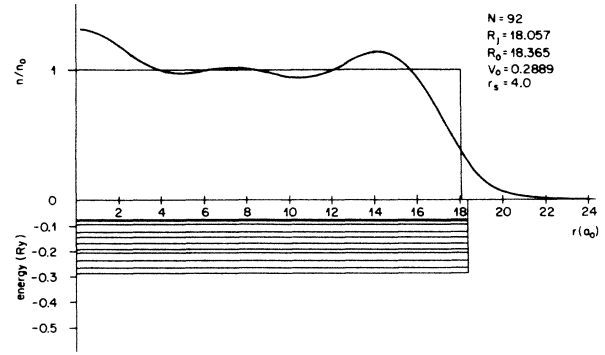

FIG. 1. Step potential minimizing the total energy of 92 electrons of sodium, $r_s=4$. The electronic density and the occupied single-electron levels are also shown, $n_0=1/(4\pi/3)r_s^3$. The energy is given by Rydberg and the radial coordinate in 1 bohr$=a_0$.

Ry and $R_0=18.805$ a.u., we found close agreement between these two and the result of that fit is shown in Table I together with the level scheme of the other potentials under study. As we see from this table, the agreement is indeed remarkably good!

Finally, we studied a potential whose parameters, $R_0=R_J$ and $V_0=100$ Ry, are thought to be representative for the classical QIB model. The reason why we did not use strictly $V_0=\infty$ is a simple numerical one. For a very large but finite step, we can use all numerical algorithms without any modification whereas in the case of $V_0=\infty$, we would have to modify the numerical work. On the other hand, it is obvious that the results for frequencies ω in the eV range are more or less the same for $V_0=100$ Ry and $V_0=\infty$.

Already a glance at the charge density of the QIB model compared to the Kohn-Sham charge density makes it clear that rather artificial results are to be expected from a *straightforward* application of this model. It was mainly for this reason that two of us (Z.P. and M. S.) ap-
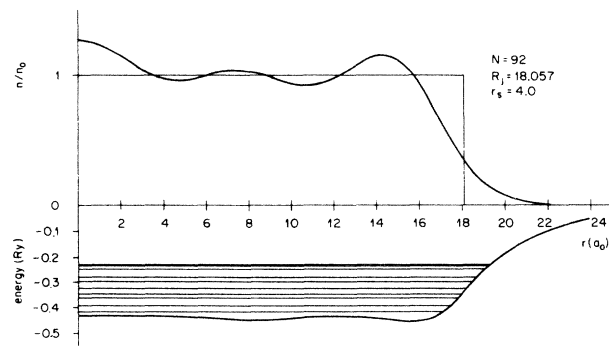

FIG. 2. Single-particle potential, charge density, and occupied electronic levels the ground state for $N=92$ and $r_s=4$, following from a completely self-consistent Kohn-Sham procedure. The size dependence of these quantities was extensively discussed in Ref. 11.

W. EKARDT, Z. PENZAR, AND M. ŠUNJIĆ

TABLE I. Single-particle levels occupied in the ground state of the various model potentials studied in this paper. All energies are given in Ry, $N=92$ electrons and $r_s=4$. ε^{KS}: Kohn-Sham result, Ref. 11, as the reference. ε^1: total-energy-minimizing step potential. ε^2: single-particle-level-scheme fixing step potential. ε^3: QIB model with $R_0=R_J$ and $V_0=100$.

l	n_l	$-\varepsilon^{KS}_{l,n_l}$	$-\varepsilon^2_{l,n_l}$	$-\varepsilon^1_{l,n_l}$	$-\varepsilon^3_{l,n_l}$
0	1	0.417 38	0.417 38	0.264 82	99.970 06
0	2	0.344 98	0.346 13	0.193 52	99.880 26
0	3	0.229 31	0.229 25	0.079 38	99.730 58
1	1	0.392 62	0.392 45	0.239 77	99.938 76
1	2	0.299 16	0.297 91	0.145 75	99.818 98
2	1	0.361 11	0.361 06	0.208 31	99.899 25
2	2	0.245 93	0.243 30	0.092 35	99.749 10
3	1	0.323 65	0.323 54	0.170 82	99.851 89
4	1	0.280 53	0.280 12	0.127 61	99.796 92
5	1	0.231 98	0.231 00	0.078 98	99.734 51

plied a *modified* QIB model to the problem of dielectric screening in small metal particles.[17] However, the problem with this modified model is that the input value of R_0 is somewhat arbitrary. It was fixed by demanding that the uppermost filled level, with respect to the bottom of the potential, agrees with the Fermi energy of the bulk metal. However, due to the size effects in small particles, that is *not* a valid criterion. Furthermore, invoking the electrostatic force sum rule[23] to adjust a certain kind of background radius $\tilde{R}_J \neq R_J$, pertaining to the choice value of R_0 is meaningless simply because this sum rule is not valid within the random-phase approximation (RPA).[24] Hence, in this paper we go back to the "classical" QIB model[16] and compare the results produced by it with those obtained from more sophisticated models. We think that, in this way, we obtain the clearest impression on the intrinsic limitations of the QIB model.

III. TDLDA FORMALISM

The application of the TDLDA formalism[9,10] was described in detail in our previous work.[1,2,4,7,8] Hence, only a very condensed summary is given in this paper.

For a detailed discussion the interested reader is referred to the work quoted above.

If the particle is placed in an external l-pole potential of the form

$$V_{\text{ex}} = -r^l P_l(\cos\theta)\epsilon_l e^{-i\omega t} , \qquad (4)$$

an induced charge density is set up which, for a spherically invariant system, has the same symmetry as V_{ex}. Within linear response the induced charge density is given as follows:

$$\rho_{\text{ind}}(r,\theta;\omega) = -\epsilon_l P_l(\cos\theta) \int_0^\infty dr'(r')^{2+l}\chi_l(r,r';\omega) . \qquad (5)$$

In Eqs. (4) and (5), ϵ_l is a (small) constant, P_l is a Legendre polynomial, and ω is the frequency.

Within TDLDA, which has the same structure as the RPAE (random-phase approximation with exchange), the l-pole density-density correlation function $\chi_l(r,r';\omega)$ is obtained as the solution of the following integral equation:

$$\chi_l(r,r';\omega) = \chi^0_l(r,r';\omega) + \int_0^\infty dr''(r'')^2\chi^0_l(r,r'';\omega)(dV_{\text{xc}}/d\rho)\chi_l(r'',r';\omega)$$

$$+ \int_0^\infty dr''(r'')^2 \int_0^\infty dr'''(r''')^2\chi^0_l(r,r'';\omega)4\pi/(2l+1)B_l(r'',r''')\chi_l(r''',r';\omega) . \qquad (6)$$

Here, χ^0_l is the corresponding independent-particle l-pole susceptibility, $dV_{\text{xc}}/d\rho$ is the density derivative of the exchange correlation potential in the ground state, and $B_l(x,y) \equiv 2x^l_< /y^{l+1}_>$. Hence, we see that as a prerequisite for the application of the TDLDA the corresponding ground-state problem must be solved first. Once it is solved, χ^0_l can be calculated as follows:[8]

$$\chi^0_l(r,r';\omega) = \sum_{l_i,n_i}^{\text{occ}} \frac{1}{2\pi} R_{l_i,n_i}(r)R_{l_i,n_i}(r')(2l_i+1) \sum_{k=0}^{\min\{l,l_i\}} \frac{a_{l-k}a_k a_{l_i-k}}{a_{l_i+l-k}} \frac{2l_i+2l-4k+1}{2l_i+2l-2k+1}$$

$$\times G_{l_i+l-2k}(r,r';\epsilon_{l_i,n_i}+\omega) + \text{c.c.}\{[\epsilon_{l_i,n_i}+\omega] \Rightarrow [\epsilon_{l_i,n_i}-\omega]\} . \qquad (7)$$

In Eq. (7), $\{l_i,n_i\}$ are the quantum numbers of the occupied single-particle states in the ground state with energy ϵ_{l_i,n_i} and wave function $R_{l_i,n_i}(r)$. The coefficients a_k are defined by $a_k=(2k-1)!!/k!$ and the retarded Green's function $G_l(r,r';E)$ can be calculated from the ground-state potential as described elsewhere.[2,7,9]

Once Eq. (6) is solved, the dynamical l-pole polarizability $\alpha_l(\omega)$ is obtained from the following equation:[8,25]

$$\alpha_l(\omega)= \int_0^\infty dr\, r^l(-1)\frac{8\pi}{2l+1}r^2$$
$$\times \int_0^\infty dr'(r')^{2+1}\chi_l(r,r';\omega)\,. \qquad (8)$$

All the information we need for the interpretation of experimental results on clusters are contained either directly in $\alpha_l(\omega)$ (for long-wavelength probes) or in $\chi_l(r,r';\omega)$. This has been shown, e.g., for electron-energy-loss experiments in Ref. 8.

IV. STATIC POLARIZABILITY

The classical l-pole polarizability of a sphere with a bulk dielectric constant $\epsilon(\omega)$ reads

$$\alpha_l(\omega)= \frac{\epsilon(\omega)-1}{\epsilon(\omega)+(l+1)/l}R^{2l+1}\,. \qquad (9)$$

If the metal dielectric constant is assumed to be given by the classical Drude form

$$\epsilon(\omega)=1-\omega_p^2/(\omega+i0^+)^2\,, \qquad (10)$$

we obtain for the static polarizability

$$\alpha_l^{cl}(0)/R^{2l+1}=1\,, \qquad (11)$$

for all values of l.

Quantum mechanically, a constant ratio of 1 is not to be expected, simply because the screening charge possesses structure which will *certainly* depend on the way it is created (e.g., the l value of the external potential). The structure of this screening charge for a Kohn-Sham barrier was discussed in detail in Refs. 1–8. In the following the results especially of Refs. 2, 7, and 8 will be used as a bench mark to estimate the value of a simplifying model potential. Quite recently the static dipole polarizability of small sodium clusters was experimentally determined by Knight *et al.*[26] The *size dependence* of the polarizability—as predicted by the spherical jellium model—agreed well with the experimental data.[26] The only difference is that the *absolute* value of the experimental polarizabilities are off by about 20%.

Figures 3(a)–3(c) show the static multipole polarizabilities $\alpha_l(0)$, in units of R^{2l+1} (continuous line), whereas the dashed-dotted line shows the l dependence of the apparent multipole surface of the sphere, δ_l, defined by[8]

$$\alpha_l(0)/R^{2l+1}\equiv(1+\delta_l/R)^{2l+1}\,. \qquad (12)$$

Hence, the underlying physics of the l dependence of the left-hand side of Eq. (12) is contained in δ_l.

Compared to the Kohn-Sham barrier, extensively discussed in Refs. 2 and 7 for $l=1$ and in Ref. 8 for $l>1$, none of the model δ_l's shows the "correct" behavior. For
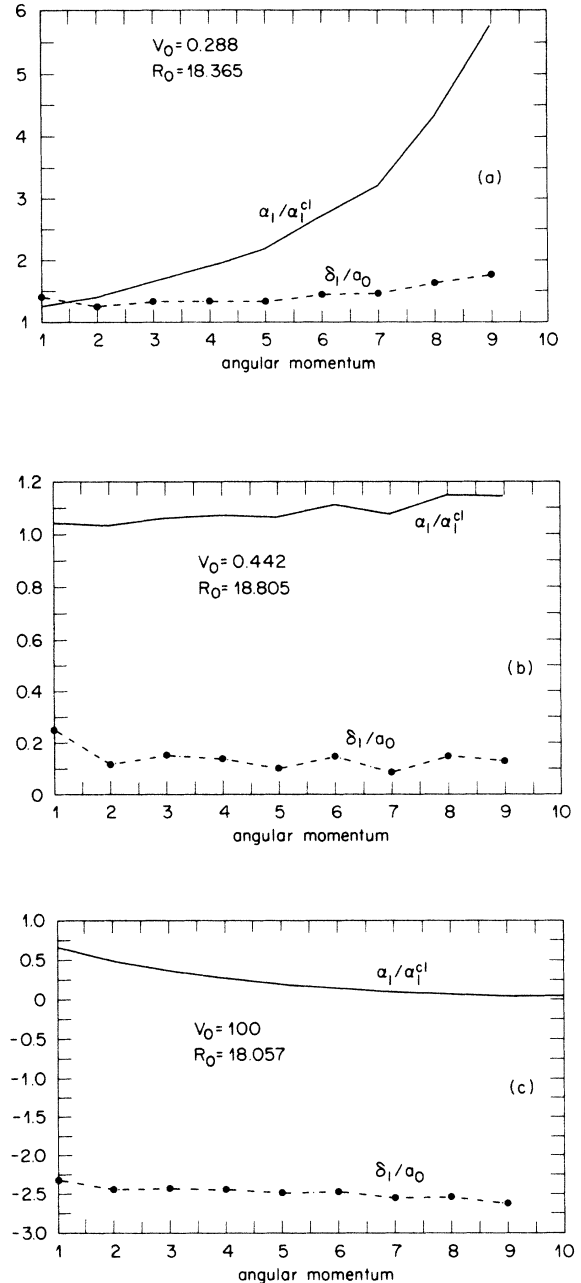

FIG. 3. Apparent multipole surface δ_l of the various model potentials [see Eq. (12)] along with α_l/α_l^{cl}. (a) Energy-minimizing step potential, (b) level-scheme fitting step potential, and (c) QIB model. Compared to the Kohn-Sham result (Refs. 2, 7, and 8) only (a) shows the correct behavior for low l values.

low l values, $l=1$ to 3, the total-energy-minimizing step potential shows approximately the correct behavior, not only qualitatively but even quantitatively. We think this is a rather interesting, new result because it shows explicitly the usefulness of a step potential *even in presence of an external field*. This gratifying feature is not attained at larger l values, which means for an external field of shorter wavelength. We believe this to be a consequence of the

shallowness of the potential which leads to the wrong description of the virtual excitation of electron-hole pairs. This result was to be expected and it was for that reason that we studied the level-scheme-fitting step potential. The result for the corresponding δ_l is shown in Fig. 3(b). δ_l behaves qualitatively correct but *quantitatively* it is now much too small. In physical terms this means that the sphere is *less* polarizable than the Kohn-Sham sphere. This is related to the fact that the potential, compared to the Kohn-Sham one, is less extended. As a consequence, the number of unoccupied bound states is smaller and, for that reason, the low-energetic highly polarizable electron-hole pairs are less numerous.

A rather strange result, compared to the other potentials, is obtained for the QIB model, shown in Fig. 3(c). Due to the artificial confinement of the electrons, the induced charge relaxes inward which makes δ_l a *negative* quantity. This is certainly an unphysical result. In the picture of virtually excited "oscillators" the reduced polarizability is mainly a consequence of the fact that both the electron-hole pairs *and* the collective surface mode are overly high in frequency. We shall explicitly confirm this picture in the next section.

V. DYNAMICAL POLARIZABILITY

We turn now to a discussion of the dynamical polarizabilities of the various model potentials. For this purpose, Eq. (6) is solved for $\omega \neq 0$ and the result is used to calculate the complex polarizability $\alpha_l(\omega)$, Eq. (8). The frequency ω is scaled with the classical surface-dipole frequency $\omega_p/\sqrt{3}$ and the calculations are performed in the range of $0.8 \leq \omega/(\omega_p/\sqrt{3}) \leq 2.4$ in steps of 0.01. We know from our earlier studies, especially from Refs. 2, 7, and 8, that this scanning is sufficient to catch all the important features and that the collective surface modes can be expected to occur in the chosen range of (0.8, 2.4). In a second calculation we did exactly the same except for replacing χ_l by χ_l^0 [see Eqs. (6) and (7)]. Upon comparing $\alpha_l^0(\omega)$ with the TDLDA-derived $\alpha_l(\omega)$, we are then able to get insight *how* the collective motion of electron-hole pairs carries characteristic features resulting from the single-particle potential confining the electronic motion.

Classically, the l dispersion of the collective surface modes, given by

$$\omega_l^{cl} = \omega_p/\sqrt{(l+1)/l+1} , \qquad (13)$$

is R-independent and exclusively a topological effect. However, we know[8] that via $q_l = l/R$ every surface mode can be assigned a wave vector which has very much the same meaning as the wave vector q, of the surface mode at a *planar* surface. For this reason the classical dispersion law Eq. (15) can be expected to change to much higher frequencies.[8] On the other hand, collective surface motion can be expected to be destroyed at an uppermost critical l value l_{cr} beyond of which the Coulomb interaction is a very weak perturbation on the independent-particle motion. All this has been verified for the Kohn-Sham barrier in Ref. 8 (for l values ranging from 1 to 10), and we are now going to do the same for the model potentials.

To begin with, we show in Figs. 4(a) and 4(b) the dynamical dipole ($l=1$) results pertaining to the total-energy-minimizing potential discussed at the beginning of this work. The dipolar dynamical polarizability is exclusively governed by two heavily damped collective features around 0.92 (surface mode) and 1.92 (volume mode). Compared to the $l=1$ Kohn-Sham results, there are *no* features due to single electron-hole pairs (in the ω region of the figure), and the width of the collective modes is much larger, which means physically a shorter lifetime. Both of these features are, of course, a direct consequence of the shallowness of the potential which especially makes Landau damping an effective decay channel for collective surface modes. That collective effects for $l=1$ are important is evident on comparing the TDLDA result with the independent-particle result. The peak position of the collective modes is correct (up to a few percent deviation), and the total oscillator strength of the surface mode seems to be very similar to the KS value. Otherwise it would hardly be understandable why $\alpha_l(0)$ compares so favorably with the corresponding KS result.

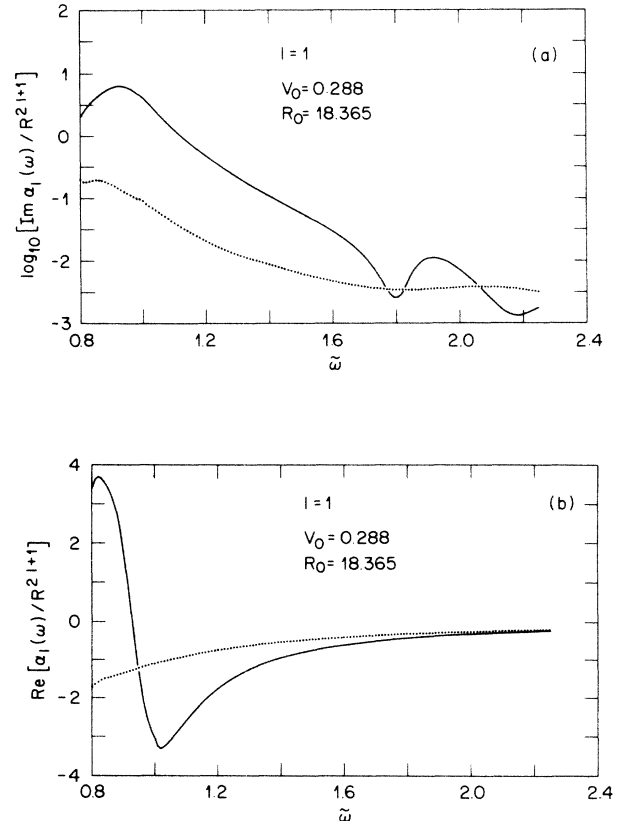Similar results are obtained for the *higher* l values (not

FIG. 4. Imaginary (a) and real (b) part, respectively, of the dynamical dipole polarizability of the step potential minimizing the total energy of the system. Continuous lines: TDLDA results, Eq. (8) of the text; dotted lines: independent-electron results. Here, χ_l^0 is used in Eq. (8). The polarizability is given in units of its static value as calculated within classical physics, namely R^{2l+1}, with R the classical (jellium) radius of the sphere.

shown). The number of electron-hole pairs is too small, the collective modes are much too broad, but their peak positions are approximately correct.

Next, we present the results for the level-scheme-fitting potential in Figs. 5(a) and 5(b). The long-wavelength response, $l=1$, consists mainly of the two collective modes. The surface mode is overly strong at the cost of particle-hole pairs which, consequently, are nearly suppressed in the spectral region shown. The peak position of the surface mode is overly high and that of the bulk overly low (both of them compared with the Kohn-Sham result). Again, similar results are obtained for the higher l values.

Finally, we show the results pertaining to the QIB model in Figs. 6(a) and 6(b). To facilitate comparison with already published QIB results of Ref. 17, the results are shown from $\omega=0$ on. Compared to all the other models, there is one striking feature: the spectrum consists solely of undamped spectral *lines*, simply because there are *no* bound-continuum transitions. For that reason, Landau damping does *not* occur in the interacting spectrum. As a consequence, both the collective surface plasmon and the collective volume plasmon are showing up as *lines* but not as *humps*. Both of the collective modes are considerably blue shifted and the oscillator strength of the surface mode is overly large (at the cost of single-pair lines). All this can be seen even more clearly
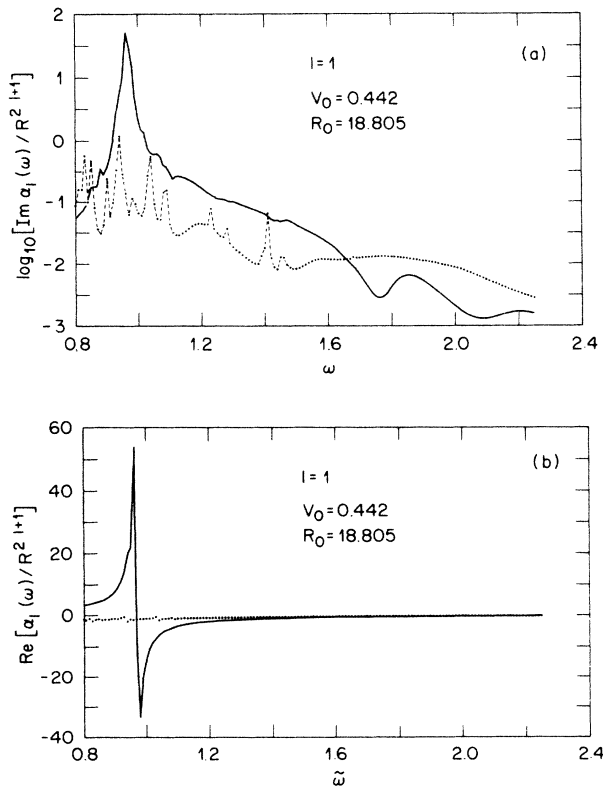

FIG. 6. Same as Fig. 4, but for the QIB model. The results are shown mainly as a demonstration for the various intrinsic flaws of the QIB model.

FIG. 5. Same as Fig. 4, but for the level-scheme fixing step potential. As expected, these curves resemble more the corresponding Kohn-Sham curves (Refs. 2, 7, and 8) but not as well as expected.
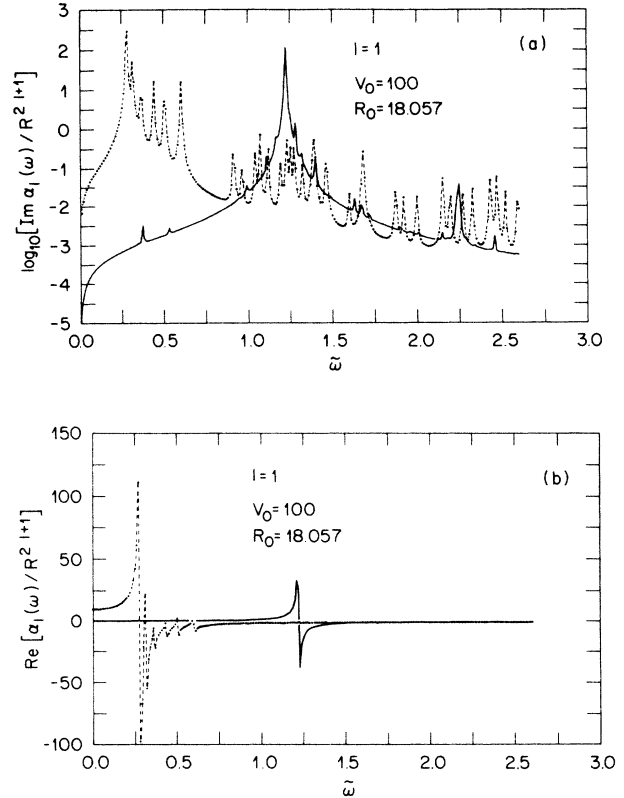
from the real part of the response function for $l=1$, which is shown in Figs. 6(b) on a *linear* scale (and not on a logarithmic one). The same artificial behavior can be seen for intermediate and high l values, not shown in the figures. There is no similarity between the dynamical behavior of the KS barrier and the QIB model, neither quantitatively nor even qualitatively. For that reason, the use of the QIB model seems to be improper even to a qualitative understanding of response phenomena at metallic surfaces.

VI. CONCLUSION

Three model potentials have been investigated aimed at a microscopic description of dielectric screening in small metal particles. If the results pertaining to a completely self-consistent Kohn-Sham-TDLDA procedure are used as a bench mark to estimate the merits of these potentials, none of the models gives satisfactory results. Only the total-energy-minimizing step potential shows static, long-wavelength screening properties comparable to the corresponding Kohn-Sham results.

[1]W. Ekardt, Ber. Bunsenges. Phys. Chem. **88**, 289 (1984).

[2]W. Ekardt, Phys. Rev. Lett. **52**, 1925 (1984).

[3]D. E. Beck, Phys. Rev. B **30**, 6935 (1984).

[4]W. Ekardt, Surf. Sci. **152**, (1985).

[5]W. Ekardt, Solid State Commun. **53**, (1985).

[6]M. J. Puska, R. M. Nieminen, and M. Manninen, Phys. Rev. B **31**, (1985).

[7]W. Ekardt, Phys. Rev. B **31**, 6360 (1985).

[8]W. Ekardt, Phys. Rev. B **32**, 1961 (1985).

[9]A. Zangwill and P. Soven, Phys. Rev. A **21**, 1561 (1980).

[10]M. J. Stott and E. Zaremba, Phys. Rev. A **21**, 12 (1980).

[11]W. Ekardt, Phys. Rev. B **29**, 1558 (1984).

[12]D. E. Beck, Solid State Commun. **49**, 381 (1984).

[13]M. Y. Chou, A. Cleland, and M. L. Cohen, Solid State Commun. **52**, 645 (1984); W. D. Knight *et al.*, Phys. Rev. Lett. **52**, 2141 (1984).

[14]B. B. Dasgupta and R. Fuchs, Phys. Rev. B **24**, 554 (1981).

[15]D. R. Penn and R. W. Rendell, Phys. Rev. B **26**, 3047 (1982).

[16]M. J. Rice, W. R. Schneider, and S. Strässler, Phys. Rev. B **8**, 474 (1973).

[17]Z. Penzar and M. Šunjić, Solid State Commun. **52**, 747 (1984).

[18]R. Ruppin, J. Opt. Soc. Am. **66**, 449 (1976).

[19]A. A. Lushnikov and A. J. Simonov, Z. Phys. **270**, 17 (1974).

[20]D. R. Snider and R. S. Sorbello, Phys. Rev. B **28**, 5702 (1983).

[21]J. H. Rose and H. B. Shore, Solid State Commun. **17**, 327 (1975).

[22]J. J. Martins, R. Car, and J. Buttet, Surf. Sci. **106**, 265 (1981).

[23]R. S. Sorbello, Solid State Commun. **48**, 989 (1983).

[24]A. Liebsch, Phys. Rev. B **32**, 6255 (1985).

[25]G. D. Mahan, Phys. Rev. A **22**, 1780 (1980).

[26]W. D. Knight, K. Clemenger, W. A. de Heer, and W. A. Saunders, Phys. Rev. B **31**, 2539 (1985).